Strontium-loaded mineral bone cements as sustained release systems : Compositions, release properties, and effects on human osteoprogenitor cells

Solène Tadier, Reine Bareille, Robin Siadous, Olivier Marsan, Cédric Charvillat, Sophie Cazalbou, Joelle Amédée, Christian Rey, Christèle Combes

Strontium-loaded mineral bone cements as sustained release systems: Compositions, release properties, and effects on human osteoprogenitor cells

Solène Tadier,[1] Reine Bareille,[2,3] Robin Siadous,[2,3] Olivier Marsan,[1] Cédric Charvillat,[1] Sophie Cazalbou,[4] Joelle Amédée,[2,3] Christian Rey,[1] Christèle Combes[1]

[1]Université de Toulouse, CIRIMAT, UPS-INPT-CNRS, ENSIACET, 4, allée Emile Monso, BP 44362, 31030 Toulouse Cedex 4, France
[2]Université de Bordeaux, Bioingénierie Tissulaire, U1026, 146 rue Léo Saignat, 33076 Bordeaux Cedex, France
[3]Inserm U1026, Bioingénierie Tissulaire, 146 rue Léo Saignat, 33076 Bordeaux Cedex, France
[4]Université de Toulouse, CIRIMAT, UPS-INPT-CNRS, Faculté de Pharmacie, 118 Route de Narbonne, 31062 Toulouse cedex 4, France

Abstract: This study aims to evaluate *in vitro* the release properties and biological behavior of original compositions of strontium (Sr)-loaded bone mineral cements. Strontium was introduced into vaterite $CaCO_3$-dicalcium phosphate dihydrate cement via two routes: as $SrCO_3$ in the solid phase (SrS cements), and as $SrCl_2$ dissolved in the liquid phase (SrL cements), leading to different cement compositions after setting. Complementary analytical techniques implemented to thoroughly investigate the release/dissolution mechanism of Sr-loaded cements at pH 7.4 and 37°C during 3 weeks revealed a sustained release of Sr and a centripetal dissolution of the more soluble phase (vaterite) limited by a diffusion process. In all cases, the initial burst of the Ca and Sr release (highest for the SrL cements) that occurred over 48 h did not have a significant effect on the expression of bone markers (alkaline phosphatase, osteocalcin), the levels of which remained overexpressed after 15 days of culture with human osteoprogenitor (HOP) cells. At the same time, proliferation of HOP cells was significantly higher on SrS cements. Interestingly, this study shows that we can optimize the sustained release of Sr^{2+}, the cement biodegradation and biological activity by controlling the route of introduction of strontium in the cement paste.

Key Words: bone cement, strontium, apatite, drug release, cell culture

How to cite this article: Tadier S, Bareille R, Siadous R, Marsan O, Charvillat C, Cazalbou S, Amédée J, Rey C, Combes C. 2012. Strontium-loaded mineral bone cements as sustained release systems: Compositions, release properties, and effects on human osteoprogenitor cells. J Biomed Mater Res Part B 2012:100B:378–390.

INTRODUCTION

Trace elements, such as sodium, magnesium, strontium, and fluoride, are naturally found in human bone.[1,2] They have attracted attention because previous studies have shown that they have an impact on bone mineral characteristics and on the biological activity of resorbable bone substitutes.[3–15] Research has particularly focused on the role played by strontium on bone formation and remineralization and it has led to therapies against bone degradation and especially against osteoporosis.[4,5,16] Strontium has been tested in different forms: carbonate, chloride, lactate, and ranelate.[4,16]

Strontium, already present in human plasma at concentrations of between 0.11 and 0.31 $\mu mol \cdot L^{-1}$, is a bone-seeking element (more than 99% of strontium is located in the bones).[3] Previous studies have shown that, at a low dose, strontium hinders osteoclast activity and favors the proliferation of osteoblast cells[3,4,11]; therefore, on the one hand it acts synergistically against osseous resorption, while on the other hand it acts by increasing the number of sites of osseous formation. Other authors have reported the stimulating action of strontium on osseous collagen formation.[3,8–11] Nevertheless, it has been shown that at higher doses, strontium can have deleterious effects on bone mineralization: mineral density and calcium absorption are both reduced.[3] High doses of strontium may also be one of the causes of the development of osteomalacia.[3,17] In addition, some authors have reported the initial and prolonged microbial inhibition of strontium-doped apatite coatings.[18]

In most cases, strontium (Sr) has been orally administered in concentrations ranging from 0.1 to 767 mg Sr/kg/day.[1,3] However, in the case of oral administration, it has been shown

Correspondence to: C. Combes; e-mail: christele.combes@ensiacet.fr

TABLE I. Composition of the Pastes of the Different Sr-Loaded Cements

	Solid Phase			Liquid Phase		Paste
	DCPD (g)	Vaterite (g)	$SrCO_3$ (g)	Deionized water (g)	$SrCl_2.6H_2O$ (g)	Wt% of Sr
Ref	1	1	0	1	0	0%
SrS	0.95	0.95	0.1	1	0	2%
SrS	0.90	0.90	0.2	1	0	4%
SrS	0.85	0.85	0.3	1	0	6%
SrS	0.80	0.80	0.4	1	0	8%
SrL	1	1	0	0.82	0.18	2%
SrL	1	1	0	0.638	0.362	4%
SrL	1	1	0	0.581	0.419	4.7%
SrL	1	1	0	0.458	0.542	6%

that even with high doses, less than 1 out of 10 Ca ions is substituted by Sr in the newly formed bone.[1] It seems that the local release of Sr from the bone substitute, directly into the osseous site, may be a solution for targeting a high turnover location while diminishing the administered strontium dose. Therefore, strontium has recently been introduced into hydroxyapatite-coatings, cements, dense or porous ceramics, and granulates.[12,13,15,18–25]

Because of its higher atomic weight compared to calcium and phosphate, strontium has also recently been proposed and studied as an interesting contrast agent for increasing the radio-opacity of calcium phosphate ceramics.[21,26]

Calcium carbonate-calcium phosphate mixed cements have been presented as a promising resorbable and injectable material for bone reconstruction.[27,28] The amount of strontium introduced into calcium-phosphate bone cement has to be optimized in order to provide both sufficient radio-opacity for the cement to be easily visualized and detected during minimally invasive surgery procedures and enough to favor bone formation without having deleterious effects on bone mineralization. However, to the best of our knowledge, no upper limit for the amount of strontium that should be incorporated into a bony defect has yet been defined.

In the present study, we investigated the introduction of strontium into a calcium carbonate-calcium phosphate cement through two different routes (Sr introduced as a mineral salt either in the solid phase or dissolved in the liquid phase) and its *in vitro* effect on cement release properties and on human osteoprogenitor cell activities in contact with these cements. Physico-chemical characterizations were performed in order to determine the effects of strontium and the way it is introduced into the self-setting paste on hardened cement composition and properties. Finally, *in vitro* assays were performed to evaluate the effect of strontium-loaded cements on the proliferation and differentiation of human osteoprogenitor cells isolated from bone marrow stromal cells to emphasize the link between strontium release and the activity of bone forming cells.

MATERIALS AND METHODS

Reactive powder synthesis

The solid phase of the reference cement (without strontium) was composed of dicalcium phosphate dihydrate (DCPD) and $CaCO_3$-vaterite (V), which were synthesized by precipitation at ambient temperature as previously described in detail.[27] Commercial strontium salts with different solubilities were purchased and used without further purification: $SrCO_3$ (Alfa Aesar®) was introduced in the solid phase and $SrCl_2.6H_2O$ (Normapur®) in the liquid phase.

Paste preparation

As previously described in detail, the reference cement paste was manually prepared by mixing equal weight of vaterite and DCPD (1:1) with deionized water as the liquid phase.[27] The liquid to solid ratio (L/S) was equal to 0.5 (w/w).

Strontium was introduced into the cement either in the solid phase or in the liquid phase by means of strontium salts with different solubilities. Considering the properties of different strontium salts (chloride, nitrate, carbonate, etc.), commercially available $SrCO_3$ and $SrCl_2.6H_2O$ were chosen to introduce Sr in the cement via the solid or via the liquid phase, respectively. In the case of $SrCO_3$, carbonate ions were already present in the reference cement; consequently no other type of counter-ions would therefore be introduced in the cement. In addition, $SrCO_3$ has a solubility close to that of vaterite $CaCO_3$ which is already present in the cement; consequently $SrCO_3$ should be resorbable. $SrCl_2.6H_2O$ salt was selected to introduce Sr in the cement via the liquid phase because of its high solubility and of the non-toxicity of counter-ions (Cl^-).

Table I details the composition of the different cement pastes: the reference cement (without strontium) is identified as "*ref*", cements where $SrCO_3$ was introduced in the solid phase as "*SrS*" and cements where $SrCl_2$ was dissolved in the liquid phase as "*SrL*".

On the one hand, varying amounts of the less soluble salt, strontium carbonate ($SrCO_3$), were added to the solid phase including the same weight ratio of vaterite and DCPD (1:1) and thus led to various weight percentages (wt%) of $SrCO_3$ in the solid phase (5, 10, 15, or 20 wt%) and consequently to various wt% of Sr in the paste (2, 4, 6, or 8%, respectively). These cements were prepared with the same L/S ratio (0.5) as the reference paste (Table I).

On the other hand, varying amounts of the more soluble salt, i.e., strontium chloride ($SrCl_2.6H_2O$), were dissolved in deionized water resulting in solutions with different concentrations in Sr^{2+} ions and viscosities. The reference solid

phase (DCPD + V; 1:1) was then mixed with the as-prepared Sr solutions, leading to pastes that were prepared with the same L/S ratio (0.5) as the reference paste, containing various wt% of Sr (2, 4, 4.7, or 6 wt%) (Table I). Note that because of the solubility of $SrCl_2.6H_2O$ in water, the maximum amount of Sr dissolved in the liquid phase and consequently included in the paste via this route was 6 wt% (compared to 8 wt% for the SrS cements).

In all cases (reference or Sr-loaded cements), the paste was then left to set in a sealed container at 37°C and in an atmosphere saturated with water (≅100% humidity). The hardened and dried cements were analyzed after maturation for four days at 37°C.

Powder and cement characterization

All of the synthesized and commercial powders and the reference and Sr-loaded hardened cements were characterized by transmission Fourier transformed infrared (FTIR) spectroscopy with KBr pellets (Nicolet 5700 spectrometer, ThermoElectron), X-ray diffraction (XRD) (Inel CPS 120 diffractometer) using a Co anticathode ($\lambda = 1.78897$ Å) and scanning electron microscopy (SEM) (LEO 435 VP microscope; silver plating of sample before observation).

A preliminary Rietveld refinement analysis was performed on SrL cement XRD patterns. The MAUD program was used to refine the lattice parameters.[29] Space groups, cell parameters, and atomic positions of the different phases: vaterite and Sr-substituted hydroxyapatite, were introduced as initial structural models.[30,31] The Caglioti function (half the width of the diffraction peaks as a function of 2θ) was evaluated using a LaB6 powder (NIST-660B). The peak shapes were fitted by using a pseudo-Voigt function. The errors on the calculated unit cell parameters were 6.10^{-3} Å for a and 3.10^{-3} Å for c.

***In vitro* release tests**

Release tests. Release tests were performed under SINK conditions on three types of set cement (reference, 8% SrS and 4.7% SrL cements) in accordance with European Pharmacopoeia specifications. A Dissolutest apparatus (Pharmatest®) containing six bowls equipped with rotating paddles (rotating speed = 100 rpm) was used. Each cylinder of hardened cement (height = 20 mm, diameter = 10.6 mm, average weight: 1.44 ± 0.05 g (ref); 1.70 ± 0.06 g (SrS); 2.4 ± 0.1 g (SrL)) was immersed for three weeks in 1 L of a buffer solution composed of 0.1*M* tris(hydroxyméthyl)aminomethane $NH_2C(CH_2OH)_3$ at physiological pH 7.4. The bowls were sealed and kept at a temperature of 37°C.

Samples of 10 mL of the working solution (buffer solution in which the cement had begun to dissolve) were removed at different times and replaced by the same volume of fresh buffer solution to keep the volume of the release medium constant throughout the experiment. The dilution factors that followed from this adjustment were considered in all calculations.

Even if no particles or very few particles were released from the cements, the solutions removed were then filtered using 0.2 μm cellulose membrane filters to remove potential particles that could dissolve during storage of the solution before analysis and which could interfere during the analysis. The filtrates were stored at +4°C before analysis. This experiment was performed in triplicate for each type of cement tested.

Characterization of the working solution. Concentrations of Ca and Sr in the working solution removed at different times were determined using atomic absorption spectroscopy (AAS) (PerkinElmer Flamme AAS, AAnalyst 400). Standard solutions from 0 to 5 ppm (linearity range for both Ca and Sr) were prepared using the same buffer solution as the one used for the release tests. Except for the samples removed at the earliest times (lowest calcium and strontium concentrations), the samples were diluted before measurements with the same buffer solution to reach the 0–5 ppm range.

Characterization of cements after release test. After three weeks in the buffer solution, the cements that had been immersed were removed from the solution and dried in an oven at 37°C. For each type of cement, two samples were manually ground and replaced in their respective working solution for an additional 24 h to determine the maximum amounts of calcium and strontium that could possibly be dissolved under these experimental conditions. The third sample was characterized by the analytical techniques indicated in the Powder and Cement Characterization section. Raman micro-spectroscopy (Labram HR 800 Horiba Jobin Yvon micro-spectrometer) and porosimetry analyses were carried also out. The total porosity of the cements was determined using a mercury intrusion porosimeter (Autopore IV 9400 Micromeritics® Instruments Inc.) with a 5 cm^3 solid penetrometer. Energy dispersive X-ray (EDX) elemental mapping was performed using a scanning electron microscope LEO 435 VP and an IMIX-PGT analyser (Princeton Gamma Tech) equipped with a Ge detector.

***In vitro* cell culture study**

Cell viability, proliferation, and differentiation were evaluated *in vitro* for the three types of cement in direct contact with human osteoprogenitor cells: the reference cement, the $SrCO_3$-loaded cement (8% SrS), and the $SrCl_2$-loaded cement (4.7% SrL). Cement disks (1 cm diameter and 4 mm thickness) were prepared and polished until smooth after the cement had set to give an even surface. The cement disks were then sterilized by γ-ray irradiation (25 KGy) before the cell culture assays.

Cell culture. Osteoprogenitor cells were isolated from human bone marrow stromal cells (HBMSCs) according to the method of Vilamitjana-Amédée *et al*. with some modifications.[32,33] Briefly, human bone marrow was obtained by aspiration from the iliac crest of healthy donors (aged 20–50 years) undergoing hip prosthesis surgery. The cells were separated into a single suspension by sequentially passing the suspension through syringes fitted with 16, 18, or 21 gauge needles. After centrifugation for 15 min at

800 g, the pellet was resuspended in Iscove Modified Dulbecco's Medium (IMDM, from Gibco, InVitrogen, Carlsbad, CA) supplemented with 10% (v/v) foetal calf serum (FCS, from Gibco) and 10^{-8} M dexamethasone (Sigma, St. Louis, MO) in order to drive the cells to the osteogenic phenotype. The cells were then placed into 75 cm^2 cell culture flasks (Nalgene Nunc, Rochester, NY), at a density of 5×10^5 cells/cm^2 and incubated in a humidified atmosphere of 95% air 5% CO_2 at 37°C. Five days later, the medium was removed, replaced twice with the complete medium supplemented with 10^{-8} M dexamethasone, and then every 3 days replaced with IMDM containing 10% FCS (v/v). Subculturing was performed using 0.2% (w/v) trypsin and 5 mM ethylenediaminetetraacetic acid (EDTA). Cell differentiation was followed at different times during cell culture by measuring alkaline phosphatase activity and osteocalcin synthesis, as previously described.[32]

Cell viability and proliferation assays. Cell viability and mortality were determined using a LIVE/DEAD viability/cytotoxicity kit, according to the manufacturer's protocol (Molecular Probes). Cell proliferation assays, quantified by MTT analysis were performed as described by Mosmann.[34] All assays were performed using at least six replicates for each condition tested. Cell proliferation on tissue culture polystyrene (TCPS) in plastic culture dishes was used as the positive control. In order to prevent cell attachment to the plastic dishes, an agarose layer (2% (v/v) in 0.1 M phosphate buffered saline (PBS at pH 7.4) was deposited in the wells, and the cement discs were placed on this layer and incubated overnight at 37°C in IMDM. Thereafter, the discs were seeded with 20×10^3 cells per cm^2 in IMDM supplemented with 10% (v/v) FCS. The cultures were incubated at 37°C in a humidified atmosphere. The culture medium was renewed every 3 days. Cell growth was quantified after 1, 3, 9, and 15 days by measuring the metabolic activity of the cells by the MTT assay. This assay is based on the observation that a mitochondrial enzyme of viable cells has the ability to metabolize a water-soluble tetrazolium dye 3-(4,5-dimethylthiazol-2-yl)-2,5-diphenyl tetrazolium bromide into an insoluble formazan salt. Briefly, 3 h after incubation of the MTT solution at 37°C, the solution was removed, the insoluble formazan crystals that had formed were dissolved in dimethylsulphoxide and 100 μL was aspirated and poured into another 96-well plate for absorbance measurements at 540 nm. The intensity of the staining obtained was directly proportional to the cell density (see AFNOR-NF EN 30993-5 and ISO 10993-5 standards). The cements were removed from the milieu after 15 days of culture, dried at 37°C and then characterized by the analytical techniques indicated in the Powder and Cement Characterization section.

The culture media that were removed after incubation, and one and nine days of cell culture were filtered through cellulose membranes and the calcium and strontium concentrations were determined by absorption spectroscopy (PerkinElmer SAA Flamme, AAnalyst 400, see the Characterization of the Working Solution section).

Cell morphology and surface characterization. After 15 days of culture, SEM observations were carried out in order to examine cell morphology on the culture discs. The samples were fixed by 15 min immersion in a 2% (v/v) glutaraldehyde in 0.15 M cacodylate buffer (pH 7.3). The samples were washed with 0.15 M cacodylate buffer for 10 min, then dehydrated by successive immersions in ethanol solutions (from 25 to 100%), and then finally dried by the CO_2 critical point technique and Au-sputtered before observation. SEM analyses were carried out at 15 and 20 keV for 60 s using a Hitachi (Tokyo, Japan) S-2500 scanning electron microscope.

Quantitative real time polymerase chain reaction (Q-PCR). Total RNA was prepared from the cells using a Machery-Nagel Nucleospin RNA extract II kit, according to the manufacturer's instructions. Adequacy of the RNA quality was assessed photometrically and by agarose gel electrophoresis.

A 1 μg weight of RNA was used as a template for single-strand cDNA synthesis using the Superscript system (Fisher Scientific) in a final volume of 20 μL containing 20 mM Tris-HCl (pH 8.4), 50 mM KCl, 2.5 mM $MgCl_2$, 0.1 mg/mL BSA, 10 mM DTT, 0.3 mM of each of dATP, dCTP, dGTP, and dTTP, 0.5 μg oligo(dT)12-18 used as a primer and 50 U of reverse transcriptase. After incubation at 42°C for 50 min, the reaction was stopped at 70°C over a period of 15 min.

A 5 μL volume of cDNA diluted at a 1:80 ratio was loaded in a 96-well plate and 20 μL of SYBR-Green Supermix (2X iQ: 50 mM KCl, 20 mM Tris-HCl (pH 8.4), 0.2 mM of each dNTP, 25 U/μL iTaq DNA polymerase, 3 mM $MgCl_2$, SYBR-Green) stabilized in sterile water was added.

Primers of ubiquitary ribosomic protein PO (forward: 5′ATGCCCAGGGAAGACAGGGC 3′-reverse: 5′CCATCAGCACC ACAGCCTTC 3′), alkaline phosphatase (ALP) (forward: 5′AG CCCTTCACTGCCATCCTGT 3′-reverse: 5′ATTCTCTCGTTCACCG CCCAC 3′) and osteocalcin (OC) (forward: ACCACATCG GCTTTCAGGAGG 3′-reverse: 5′GGGCAAGGGCAAGGGGAAGAG3′) were used at the final concentration of 200 nM.

The data were analyzed with the iCycler iQ software and compared using the ΔΔCt method. Each Q-PCR was performed in triplicate for PCR yield validation. The data were normalized to PO mRNA expression for each condition. We have chosen P0 as the reference or housekeeping gene that encodes for a ribosomal protein and which is not influenced by the experimental conditions. The results were thereafter normalized to the expression of the corresponding gene, expressed by the cells cultured on the plastic culture dishes (that represent one as relative value). Statistical significance was calculated by Student's *t*-test.

RESULTS

Sr-loaded cement characterization

All compositions of the Sr-loaded pastes that were tested (Table I) led to hardened cements. The set reference cement was composed of vaterite and nanocrystalline apatite which was shown to be carbonated in a previous paper.[27] X-ray diffraction analysis [Figure 1(a)] of the set cements showed that when $SrCO_3$ was included in the solid phase it remained in the final cement, thus the composition was

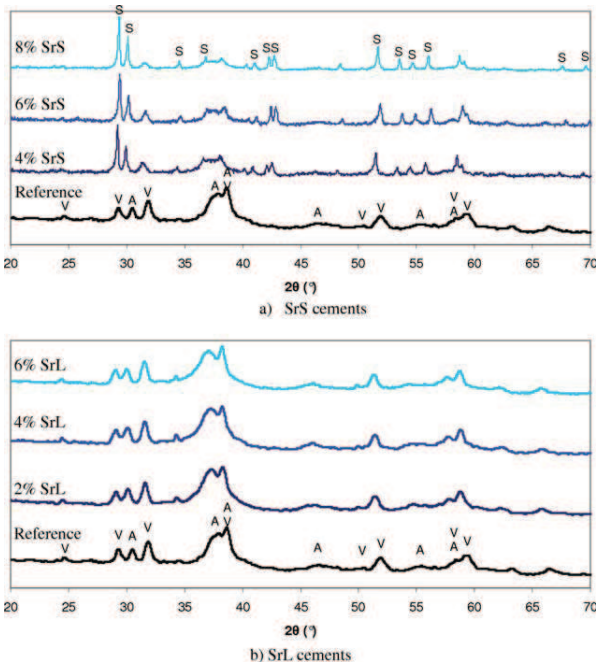

FIGURE 1. X-ray diffraction patterns of the different Sr-loaded set cements: (a) SrS cement; (b) SrL cement. V: $CaCO_3$ – vaterite; A: nanocrystalline apatite; S: $SrCO_3$. [Color figure can be viewed in the online issue, which is available at wileyonlinelibrary.com.]

comprised of carbonated apatite, vaterite, and strontianite ($SrCO_3$). The relative intensity of the diffraction peaks of strontianite clearly increased as the initial load of $SrCO_3$ increased indicating that this compound did not have a significant part in the setting reaction. When strontium chloride was introduced into the paste via the liquid phase, no additional phase was detected compared to the reference cement [Figure 1(b)]. The preliminary Rietveld refinement analysis of cement XRD diagrams enabled the determination of apatite cell parameters as a function of Sr-loading in the liquid phase and thus in the cement paste; the evolution of these parameters can be observed in Figure 2 and compared with the Vegard's law, as described by Leroux et al., for partly substituted apatite $Ca_{10-x}Sr_x(PO_4)_6(OH)_2$.[35] Considering the study of Leroux et al., we can see that the a

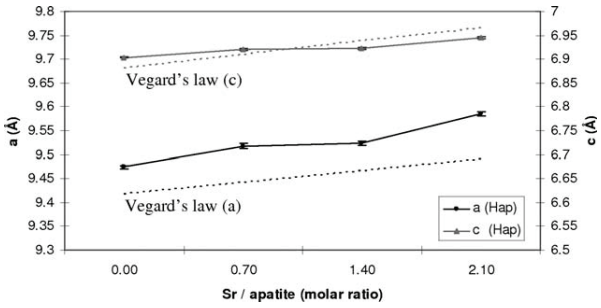

FIGURE 2. Hydroxyapatite (Hap) cell parameters (a,c) as a function of Sr load compared with (a) and (c) Vegard's law (dotted lines) according to Leroux *et al.*[35]

TABLE II. Total Porosity (%) of the Three Types of Cements Before and After the *In Vitro* Release Test (3 Weeks)

	Reference Cement	8% SrS Cement	4.7% SrL Cement
Before release test	61 ± 1	49 ± 1	52 ± 2
After release test	69 ± 2	63 ± 2	68 ± 2

parameter is higher than expected and that the c parameter has a lower increase than expected. We can also note that the increase in the c lattice parameter of the apatite formed after setting is visually confirmed by the shift of the 002 line of apatite at about $2\theta = 30–31°$ toward lower 2θ values as Sr introduced in the liquid phase increased [see Figure 1(b)]. The 00l lines of apatites are rather narrow and the variation of the c parameter reported is more reliable and significant than that for the a parameter.

The total porosity of the different Sr-loaded cements is reported in Table II. The introduction of strontium into the cement formulation led to a decrease of about 10% of the total porosity compared with the total porosity of the reference cement. Upon examining the pore size distribution (Figure 3) for the different Sr-loaded cements that were prepared, it could be seen that when strontium was

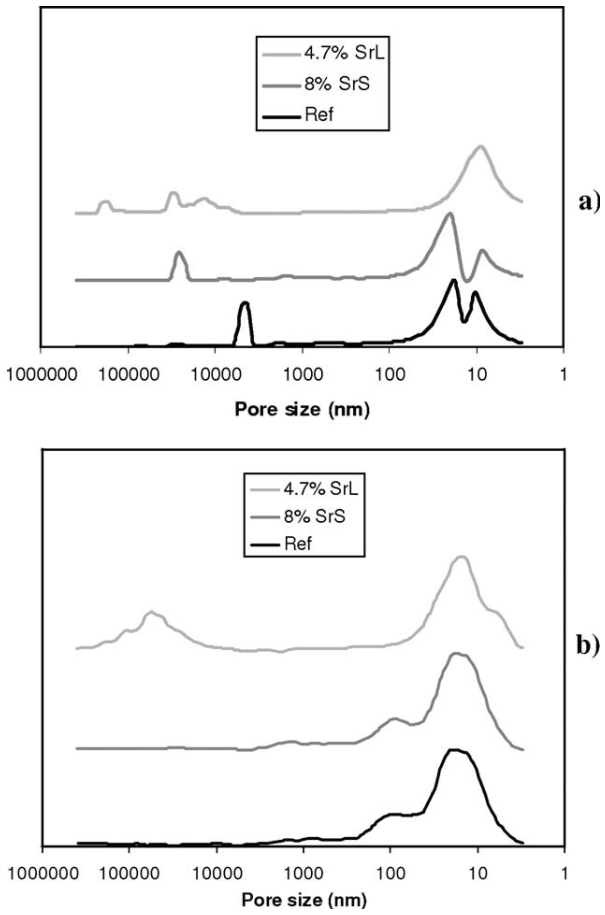

FIGURE 3. Pore size distribution of the three types of cement before (a) and after (b) the *in vitro* release test.

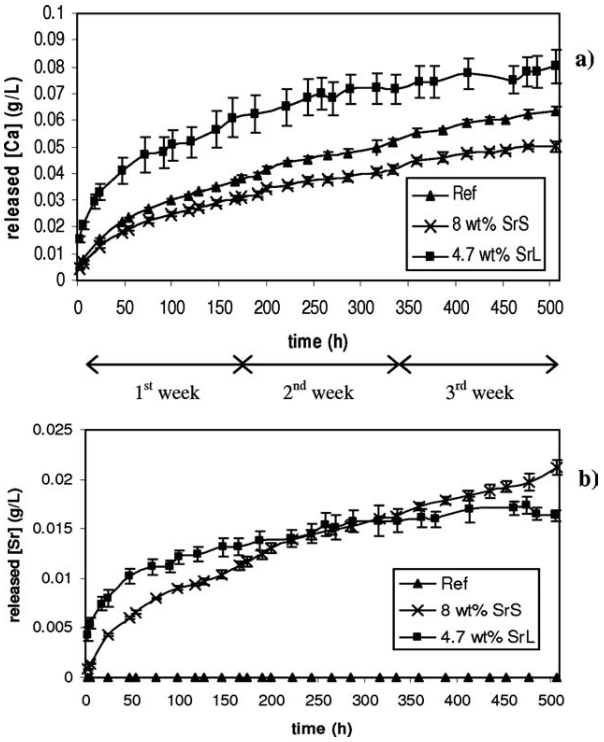

FIGURE 4. Concentrations of calcium and strontium released from the different cements tested in the working solution as a function of time: (a) Ca released from: (i) reference cement; (ii) $SrCO_3$-loaded cement (SrS) including 8 wt% Sr in the paste; (iii) SrL including 4.7 wt% Sr in the paste (b) Sr released from: (i) reference cement; (ii) $SrCO_3$-loaded cement (SrS) including 8 wt% Sr in the paste; (iii) SrL including 4.7 wt% Sr in the paste. Data shown are mean ± SD ($n = 3$).

introduced into the cement formulation, either in the solid or liquid phase, the size of the bigger pores increased (for example, from 4 to 26 μm for 8% SrS cement). It is important to note that for all of the cements the nanosized pores played a prominent role in the total porosity of the cement (in the case of 8% SrS cement with a total porosity of 49%: 45% by the pores of an average size of 8 and 20 nm compared to a contribution of 4% by pores of an average size of 25 μm).

Strontium and calcium release *in vitro*

The concentrations of calcium and strontium ions released from the different cements tested in the working solution are plotted against time in Figure 4. Regarding calcium release [Figure 4(a)], all of the cement types showed the same trend: even though the SrL cements showed a higher release rate, calcium was continuously released from the cements, with a faster rate of release during the first 50 h and slower afterward. The cumulated Ca concentration in the working solution after 3 weeks reached 0.06 g/L for the reference cement, 0.05 g/L for 8% SrS, and 0.08 g/L for the 4.7% SrL cement (values normalized per gram of cement that was initially introduced into the working solution).

Regarding strontium release [Figure 4(b)], both Sr-loaded cements showed different trends. Although it contained less strontium, the amount of strontium released from the SrL cement was higher than that from the SrS cement during the first 50 h. Then the rate of strontium release slowed down and reached similar or lower rates than SrS cement after one week in solution. After 3 weeks of being tested in the release solution, the cumulated Sr concentration in solution reached 0.021 g/L for 8% SrS cement and 0.016 g/L for SrL cement (values normalized per gram of cement that was initially introduced into the working solution).

In order to determine the mechanism of Sr release and the dissolution of the cements, it was important to characterize the cements after the *in vitro* tests in the presence or absence of cells: X-ray diffraction analysis provided the global composition of the cement, whereas Raman microspectroscopy provided the local one.

Figure 5 presents the XRD diagrams of the three types of cement blocks after the *in vitro* tests: (i) as removed from the working solution after 3 weeks [Figure 5(a)]; (ii) removed from the working solution after 3 weeks, manually ground in a mortar, and replaced as powders in their respective working solutions for an additional 24 h [Figure 5(b)]; (iii) after 15 days of the cell culture test [Figure 5(c)]. By comparing Figures 1 and 5, we can see that the composition of the cement blocks was similar before (Figure 1) and after the *in vitro* tests in both the absence and presence of cells

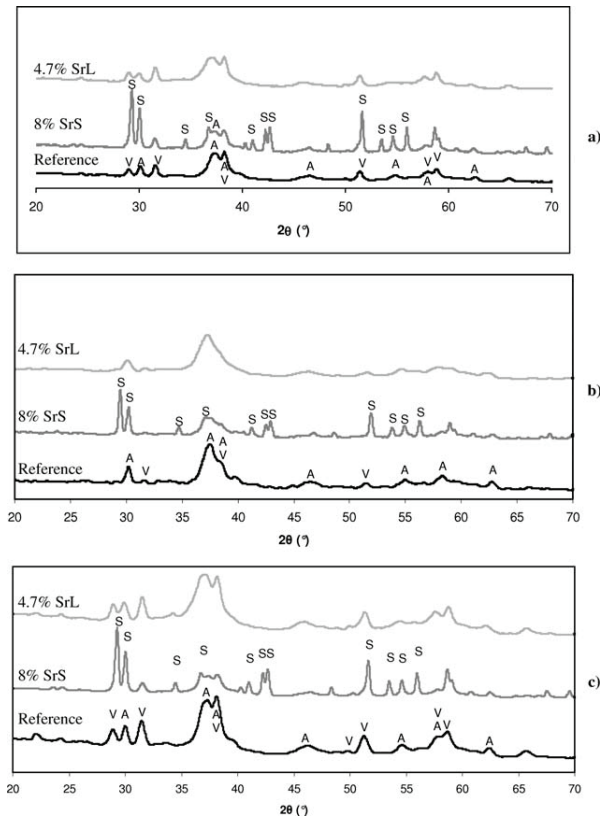

FIGURE 5. X-ray diffraction patterns of the three types of cement: (a) after 3 weeks of the *in vitro* release test; (b) after the *in vitro* release test for 3 weeks as a cement block and one more day as ground powder; (c) after 15 days of the *in vitro* cell culture.

[Figure 5(a,c), respectively]: vaterite remained in the three types of cements either after three weeks in buffered solution or after two weeks in contact with culture medium and cells. However, a significant difference can be clearly observed for the XRD patterns of the cement powders replaced in the working solution for an additional 24 h [Figure 5(b)]: the diffraction peaks characteristic of vaterite are no longer visible on the XRD pattern of the SrS cement and they are of a very low intensity for the reference and SrL cements. This indicates that the vaterite, which remained in the cement blocks after 3 weeks, dissolved within 24 h when the blocks were ground into powders. The resulting SrL cement consisted of a poorly crystallized apatite showing broader and less well resolved peaks than SrS or the reference cement. In the case of the SrS cement, it can be noted that nanocrystalline apatite co-existed with the well-crystallized $SrCO_3$, which remained in the cement after the release test regardless of the form of the cement (block or powder). This result indicated that strontianite ($SrCO_3$) was stable in the Tris buffer solution at pH 7.4 and 37°C. However, in order to further investigate the composition of these cements after the 3-week release test, we performed elemental mapping by EDX and Raman micro-spectroscopy analyses on a cross-section of the cement cylinders.

Elemental mapping of the three types of cement was performed for calcium, phosphorus, and strontium (Figure 6). In particular, the phosphorus maps revealed heterogeneity in the composition with a brighter peripheral layer indicating a relatively higher concentration of phosphorus than in the center of the cement. However, this P-rich peripheral layer was less marked for the SrL cement. Upon examination of the strontium maps, it could be seen that this element was homogeneously distributed within the SrL cement, supporting the hypothesis of the incorporation of Sr in the apatite lattice, whereas for the SrS cement some brighter spots indicated the presence of $SrCO_3$ agglomerates that were not homogeneously distributed. In addition a brighter peripheral layer can be distinguished for the SrL cement indicating a relatively higher concentration in strontium than in the center of the cement probably due to the preferential dissolution of vaterite in this zone thus mainly consisting of strontium-substituted apatite.

Figure 7 shows the spectra of the SrS cement after 3 weeks of *in vitro* release test compared with spectra of the reference compounds (vaterite, $SrCO_3$, and the carbonated apatite analogous to bone mineral). The spectrum of the edge of the cement cylinder mainly shows the characteristic band of the phosphate groups in carbonated apatite (960 cm^{-1}); a low intensity band at 1070 cm^{-1} indicating the presence of $SrCO_3$ could also be distinguished. Note that this band was superimposed on the band of very low intensity at 1070 cm^{-1}, characteristic of phosphate groups in carbonated apatite. This spectrum was completely different from the one obtained when the center of the cement was analyzed, where intense bands characteristic of carbonate groups in vaterite (1075–1090 cm^{-1}) and $SrCO_3$ (1070 cm^{-1}) were seen, along with a less intense band characteristic of phosphate groups in carbonated apatite. This Raman spectroscopy data confirmed the EDX spectroscopic data (Figure 6).

Upon comparing the total porosity of the cements before and after the release test (Table II), it can be seen that it was significantly higher after the *in vitro* test: this increase was more important for the Sr-loaded cements.

Examination of the pore size distribution after the *in vitro* release test suggested the formation of a secondary porosity during cement degradation *in vitro* [Figure 3(b)]. The pore size distribution around 10 nm, which was bimodal before the test for the reference and SrS cements, became monomodal and broader toward the higher pore sizes; pores of about 100 nm were created. In addition, after the release test, the SrL cements presented a secondary pore size distribution (around 8 nm) of smaller pore sizes than before the test. A broadening of the pore size distribution toward higher pore sizes was noted for the SrS and SrL cements. This result could have been due to degradation of the cements, and particularly to the dissolution of vaterite $CaCO_3$ and $SrCO_3$.

In vitro cell culture study

Results were obtained from three separate experiments that used human osteoprogenitor cell cultures arising from three different donors of bone marrow. Figure 8 shows that the cells seeded on Sr-loaded cements exhibited the same profile of proliferation from day 1 to day 9 of culture as for the reference cement. However, the rate of proliferation remained significantly lower on these materials than on the plastic culture dishes, especially at day 9 and day 15. After 15 days of culture, it was noted that the human osteoprogenitor cells showed a more significant proliferation on SrS cement than on either the reference or the SrL cements.

Live/dead assays performed on the three types of cements [Figure 9(d–f)] mainly revealed living cells on these three surfaces. This analysis was corroborated by a SEM examination [Figure 9(a–c)], which showed cells that were well spread out with numerous filopodia, regardless of the substrate (reference, SrL, or SrS cements).

Q-PCR was performed to quantify the mRNA levels of the early bone-specific marker (alkaline phosphatase) and the later bone-specific marker (osteocalcin) after 15 days of culturing the human osteoprogenitor cells on the three cement types (reference, SrL and SrS) and on the plastic culture dishes as control (Figure 10). The expression of ALP mRNA levels in cells cultured on these three cements did not differ, regardless of whether the cement was loaded with strontium or not. The same result was obtained for the late osteoblastic marker osteocalcin, which was not significantly regulated by the presence of strontium within the cements. However, the expression of these two bone markers was overexpressed in cells cultured on the three types of cements in comparison with the control surfaces (plastic culture dishes), regardless of the presence of strontium within the cements (Figure 10).

The concentrations of strontium and calcium released into the culture medium after the overnight incubation of the cements, after 1 and 9 days of cell culture, are presented in Figure 11. A burst of release of strontium and calcium occurred during incubation and on the first day of cell culture for the 4.7% SrL cement, whereas their release was moderate at 9 days of cell culture. The calcium release rate for 8% SrS

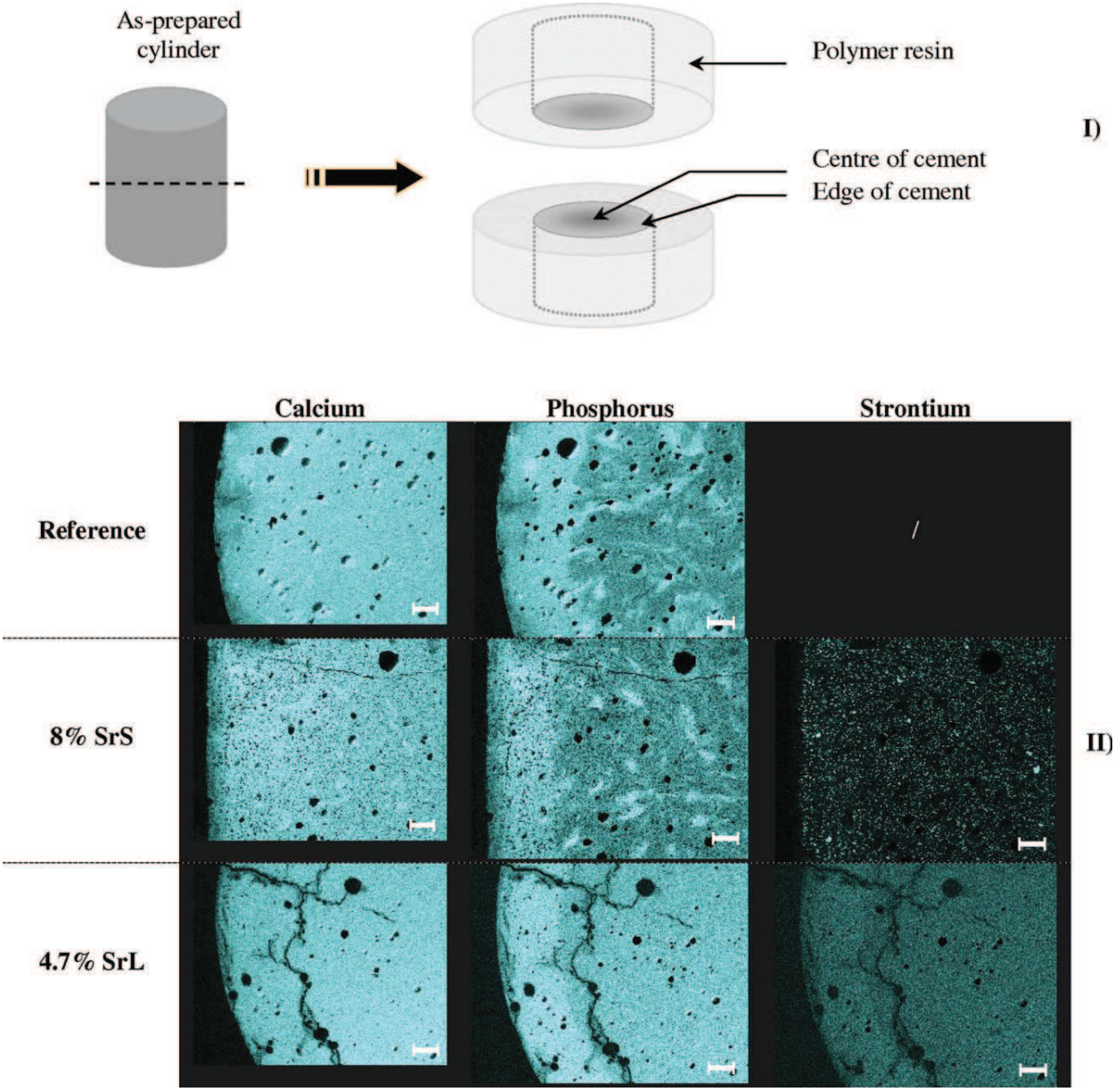

FIGURE 6. EDX elemental mapping (Ca, P, and Sr) of the three types of cement after three weeks of the release test. (I) Preparation of the sample; (II) Ca, P and Sr elemental maps (magnification: ×25; scale bar = 400 μm; brighter points: higher concentration of the element). [Color figure can be viewed in the online issue, which is available at wileyonlinelibrary.com.]

cement was quite similar to that of the reference cement [Figure 11(a)]. The calcium and strontium release rates for the 8% SrS cement were very low compared with those of the 4.7% SrL cement, indicating a different bioavailability of strontium and cement biodegradation properties depending on the Sr-loading route chosen for the cement.

DISCUSSION

Sr-loaded cement compositions and properties

Several authors have investigated various routes for introducing strontium into apatite or brushite bone cements and a commercial cement formulation includes strontium carbonate.[8,23,26,36–39] In all cases, strontium was introduced in the solid phase. In the present study, we investigated the introduction of strontium in solid and liquid phases and the feasibility of both types of self-setting pastes was demonstrated. Interestingly, the two different routes used to introduce strontium into the cement led to two different compositions of cements: when $SrCO_3$ was included in the solid phase it remained in the final cement composition, whereas when $SrCl_2$ was dissolved in the liquid phase Sr^{2+} ions were readily available in the paste and could be incorporated into the apatite phase during the setting reaction by substituting Ca^{2+} ions and consequently no additional phase

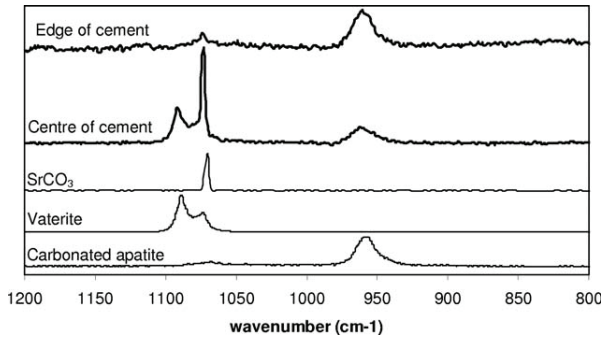

FIGURE 7. Raman spectra of the reference compounds and of two zones of the 8% SrS cement after three weeks of the *in vitro* release test.

was detected compared with the reference cement. Variations in a and c parameters of the apatite lattice were also reported by Wang et al. as a function of the Sr/(Ca+Sr) molar ratio when two routes of introduction of strontium in the solid phase of amorphous calcium phosphate and DCPD cement were investigated.[39] The variation they reported for the c parameter was higher (higher slope) than shown in Figure 2 of the present study and was thus closer to that reported by Leroux et al.[35] The lower increase of c parameter observed in the present study (Figure 2) could be due to the concomitant substitution by strontium and chloride (from $SrCl_2$ salt dissolved in the liquid phase) in the apatite. Indeed the effect of Sr on the crystallographic parameters of apatite is rather large, especially on the c dimension, whereas chlorine incorporation would have an opposite effect on this dimension. In addition the 00l lines are rather narrow due to elongated shape of the apatite crystals and the variation reported is significant. These simple considerations support the data obtained by our preliminary Rietveldt refinement analysis, considering also that the atomic diffusion coefficient of Sr is much larger than that of Ca and that even small amounts of Sr incorporation are quite observable on XRD data as shown by several authors.[11,39,41] However, it is important to note that in the present study, the possibility of having concomitant substitution of calcium by strontium and hydroxide by chloride, the coexistence of various degrees of substitution into the apatite formed in the SrL cement and its low crystallinity did not allow us to obtain reliable quantitative information on the amount of strontium incorporated in the apatite lattice. Considering the work of O'Donnell et al. Raman spectroscopy can also be useful to identify and quantify Sr substitution in hydroxyapatite: the position of the ν_1PO_4 band in hydroxyapatite (961 cm^{-1}) decreased linearly for Sr-substituted hydroxyapatites and the full width at half maximum of this band can well correlated and increased linearly with increasing crystallite size calculated by XRD analysis.[40]

These various cement compositions should lead to different behaviors of the cement in solution considering the solubility of hydroxyapatite and of Sr-substituted hydroxyapatite. Indeed, the different crystallization and dissolution properties of such apatites should determine the setting of the cement (formation of apatite) and its biodegradation and release properties. Christoffersen et al. reported the inhibitory role of strontium on the rates of dissolution and crystal growth of hydroxyapatite and 10% Sr-containing hydroxyapatite; the latter was less affected than the former.[41]

Our results showed that partially substituted Sr-hydroxyapatite was formed in SrL cements and that early high rates of released calcium and strontium were detected when the SrL cement was tested *in vitro* in both the presence and absence of osteoprogenitor cells, whereas the SrS cement, which was mainly composed of hydroxyapatite, showed a relatively moderate release of ions. It is now interesting to discuss the release and dissolution properties of these cements.

Release and dissolution properties of strontium-loaded cements

Several studies reported associations between calcium phosphate bone cements and drugs (antibiotics, bisphosphonates, and growth factors, for example) as *in situ* drug release systems.[42–46] However, very few studies investigated strontium release from Sr-loaded cements.[13,20] Alkhraisat et al. investigated strontium release at 37°C in pure water in dynamic conditions (water refreshed daily) for brushite cements prepared with a solid phase including strontium-substituted tricalcium phosphate.[13]

In the present work, we studied strontium release in a buffered solution at pH 7.4 and 37°C over a period of 3 weeks. For both types of Sr-loaded cements, we observed a sustained release of strontium for 3 weeks in both the presence and absence of osteoprogenitor cells, including an initial burst of release of Ca and Sr during the first 48 h (Figures 4 and 11). After an initial period (24 h for the SrS cement), the ratio of the Ca/Sr released then stabilized at around 2.5 and remained constant throughout the rest of the experiment. Note that the Ca/Sr ratio in the cement paste was 2.1 and that the Ca/Sr ratio released was therefore higher. We can hypothesize that the $CaCO_3$-vaterite, which remained in the cement after the setting reaction (Figure 1), and which is the more soluble phase, dissolved first, explaining the high Ca/Sr ratio during the first couple of days. Then, $SrCO_3$ also began to dissolve, which explains the decrease in the Ca/Sr ratio.

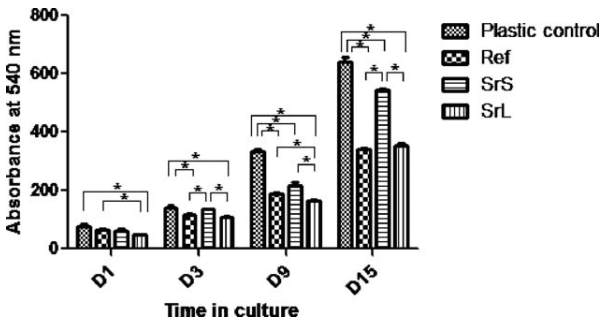

FIGURE 8. Cell proliferation of human osteoprogenitor cells cultured on the three cements for 15 days, quantified by MTT assays. Data shown are mean ± SD of triplicate experiments for each series (* $p \leq 0.05$).

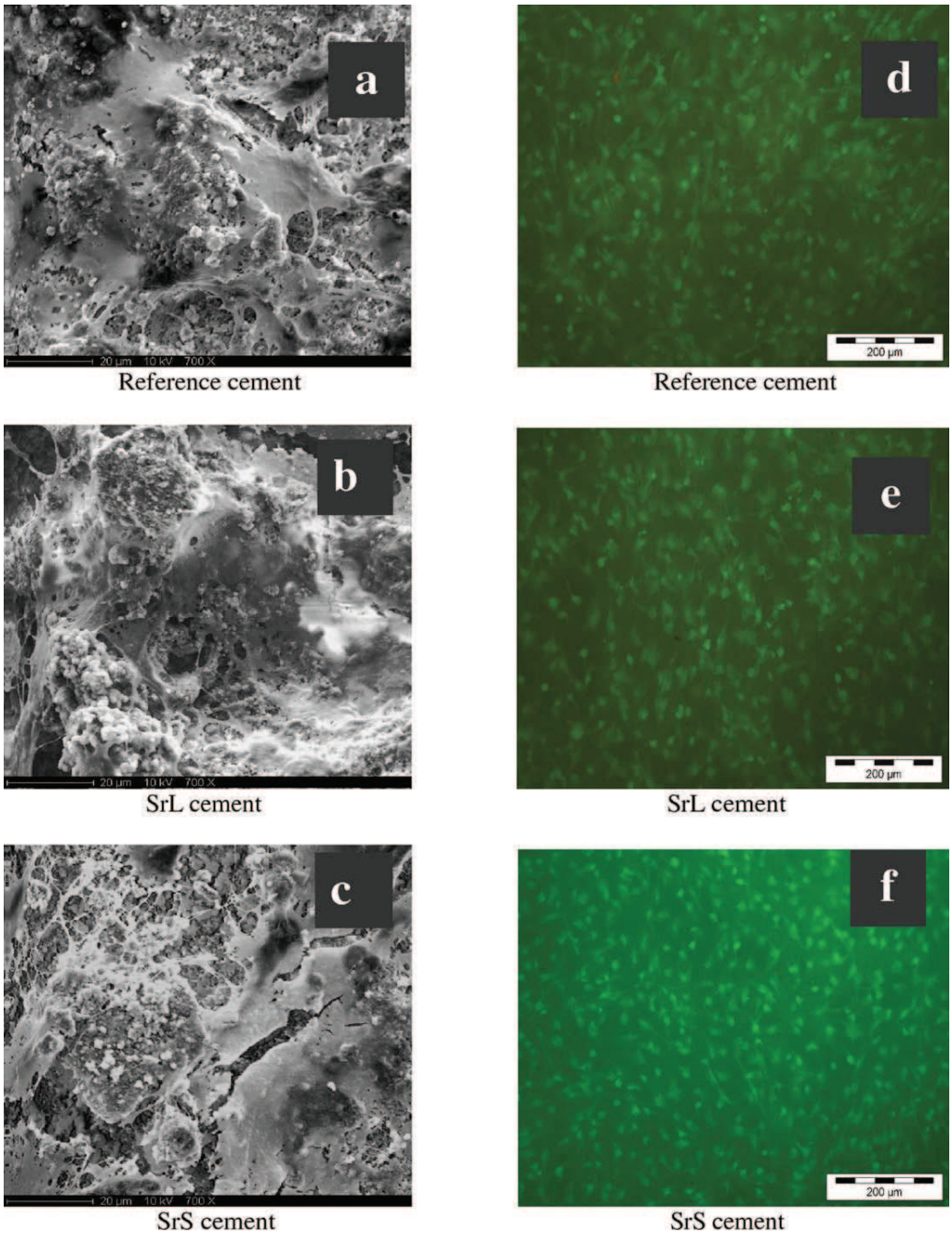

FIGURE 9. SEM micrographs of cement surfaces after 15 days of culturing human osteoprogenitor cells: (a) reference, (b) SrL and (c) SrS cements. Live/dead assays were performed after 15 days of cell cultures: (d) reference, (e) SrL and (f) SrS cements. [Color figure can be viewed in the online issue, which is available at wileyonlinelibrary.com.]

The EDX elemental mapping revealed a relative increase in phosphorus in the peripheral layer of all the cement blocks, which confirms the hypothesis of the early dissolution of vaterite $CaCO_3$ and consequently a relative enrichment of the less soluble apatite in the peripheral layer (Figure 6). This less soluble peripheral layer could constitute a barrier that would slow down the dissolution of vaterite from the core of the cement. However, this effect could be partially compensated for by the formation of a secondary porosity that could facilitate the diffusion process. The Raman micro-spectroscopy analysis performed on two regions of the SrS cement cylinder (edge and center, Figure 6) after the release test confirmed the dissolution of vaterite on the edge, suggesting that the vaterite dissolution process was limited by diffusion during the *in vitro* test. In addition, the centripetal dissolution of vaterite was confirmed

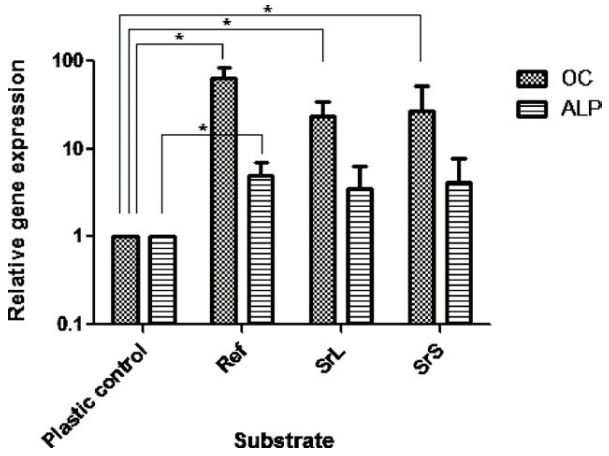

FIGURE 10. Relative mRNA expression levels of alkaline phosphatase (ALP) and osteocalcin (OC) in human osteoprogenitor cells cultured for 15 days on the three cements (Ref, SrL, and SrS cements) and on plastic culture dishes as the control. Data of gene expression was quantified relative to gene expression of the same cells cultured on plastic dishes after the same time of culture.

by comparing the results of the X-ray diffraction analysis on blocks and powders (ground cement blocks) removed after the *in vitro* release tests [Figure 5(a,b)]. As diffusion is a less limiting process for cement dissolution when in the form of a powder compared to a block, vaterite was almost completely dissolved within 24 h when the ground cement was tested in the release solution [Figure 5(b)].

In the case of 4.7% SrL cement, the release of calcium and strontium was very high during incubation and the first day of cell culture (Figure 11), in correlation with the results of the *in vitro* release test (Figure 4). This initial burst of release could have slightly reduced cell proliferation in comparison with the SrS and reference cements (Figure 8).

However, in all cases, the daily doses of strontium released per gram of cement (for example, for the 4.7% SrL

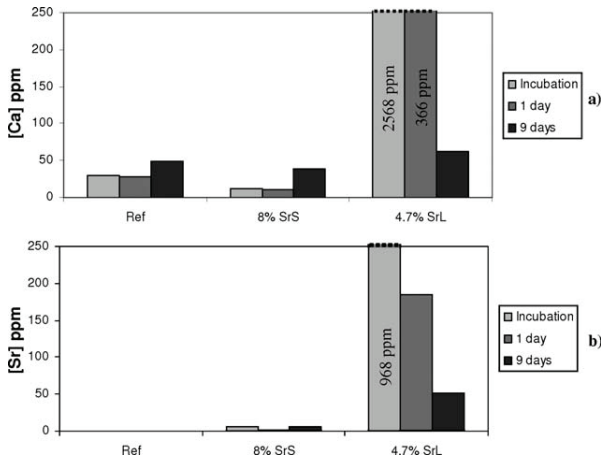

FIGURE 11. Calcium (a) and strontium (b) concentrations in the culture medium at different times before and during cell culture on the three types of cement.

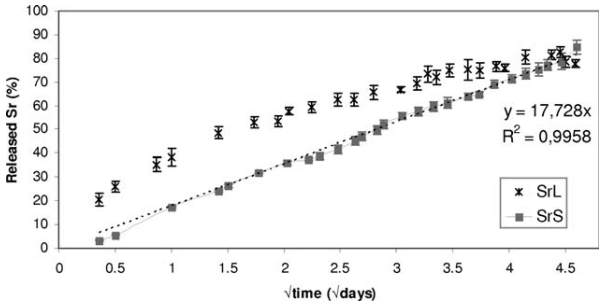

FIGURE 12. Representation of the release kinetics according to the Higuchi model. Data shown are mean ± SD ($n = 3$).

cement: 8 mg during the first day of the release test and 0.5 mg during the third week) were lower than the therapeutic doses used for oral administration and in the same order of magnitude as the *in situ* dose proposed by Alkhraisat (i.e., between 12 and 30 mg Sr/L).[3,13] However, it is difficult to compare these two therapeutic routes (*in situ* or oral administration) in terms of Sr level distribution locally around the cement/bone defect and generally in circulating blood.

Contrary to what was observed for the SrS cement, the ratio of the Ca/Sr released rapidly stabilized at around 4.6 for the SrL cement, which exactly corresponded with the initial Ca/Sr molar ratio (in the cement paste). This result may indicate that the release mechanisms of SrS and SrL cements are different. In order to investigate this point further, the release kinetics shown in Figure 4(a,b) were modeled. If release/dissolution kinetics fit the Higuchi model, this indicates that diffusion is the main mechanism involved in the release of the drug.[47] The Higuchi model links the percentage of the drug released, Q, to the time, t, and k, a rate constant, as defined in the following equation: $Q = k\ t^{1/2}$. Figure 12 shows that the evolution of Q as a function of $t^{1/2}$ for the release of strontium from the 8% SrS and 4.7% SrL cements was linear for the SrS cement and non-linear for the SrL cement. These results suggest that for the SrS cement, strontium was released by diffusion through the porous network created by the water inside the cement, whereas such a mechanism was not involved or not predominant for the SrL cement. In this latter case, the release of strontium may have been limited by the dissolution of Sr-substituted apatite or its degradation when in the presence of cells. This hypothesis was supported by Raman micro-spectroscopy and EDX elemental mapping analyses (Figures 6 and 7). Moreover, the results obtained with the mercury porosimeter highlighted the creation of a secondary porous network for the SrS and SrL cements, which could have been due to water diffusion into the cement.

Another parameter that could have been involved in the higher release and dissolution rates of SrL cements during the first week is related to the higher initial porosity of these cements. According to the work of Cazalbou et al., the surface of nanocrystalline biomimetic apatite which is formed during cement setting can undergo fast Ca-Sr cationic exchanges depending on the composition of the solution, which could

have contributed to the initial burst of release of Sr that we observed *in vitro*.[1,48]

Finally, another parameter involved in the release process was the solubility of the apatite formed during the cement setting reaction. The greater release of Sr and Ca from the SrL cement is in agreement with the increase in solubility with the increasing content of Sr^{2+} in the apatite crystal.[41,49] Interestingly, these results suggest that it is possible to control the release of Sr^{2+} and the biodegradation of the cement by the method used to introduce strontium into the cement paste.

Previous studies performed on Sr-loaded biomaterials showed that the proliferation and differentiation of cells is Sr-dose dependent.[9,14,25] Therefore, a possible correlation between the release/dissolution properties on the proliferation and differentiation of osteoprogenitor cells is discussed in the next paragraph.

Effect of Sr-loaded cements on osteoblast cell activity

Several recent works investigated the effect of strontium from Sr-doped mineral cements, coatings, and ceramics on cell proliferation and differentiation.[8–14,24,25,37]

Alkhraisat et al. showed that cytocompatibility of Sr-containing brushite cements was as good as that of reference brushite cements (without Sr) via culturing the human osteoblast cell line hFOB1.19.[13] In addition, two cell lines were tested on Sr-containing brushite cements by Pina et al.: their results showed the stimulation of pre-osteoblastic proliferation and osteoblastic maturation of MC3T3-E1 cells and non-cytotoxicity toward human osteosarcoma-derived MG63 cells.[8]

In our study, regardless of the composition of cement tested, the human bone marrow stromal cells showed similar proliferation profiles up to 9 days of culture. After this, cell proliferation was 50% higher on the SrS cement compared to reference and SrL cements (Figure 8). The correlation between the results of cell proliferation (Figure 8) and Sr release *in vitro* in the absence (Figure 4) and presence of cells (Figure 11) suggested that the early released dose of strontium had a determinant role on cell proliferation. Braux and coworkers have recently determined the optimal range of $SrCl_2$ concentration in solution (between 10^{-5} and 10^{-4} M) to enhance primary bone cell proliferation.[9] This range of strontium concentrations is lower compared with the strontium concentrations measured in the culture medium during cell culture on the three types of cement (Figure 11).

The promoter role of the three types of cement was confirmed by examining the high level of differentiation in gene expression in comparison with the plastic culture dishes. However, it appeared that strontium did not stimulate the expression of the early bone marker (alkaline phosphatase), or the late osteoblastic marker (osteocalcin). It is important to note that titration of the Sr and Ca released in the cell culture medium as a function of time revealed that the incubation of Sr-loaded cements in IMDM medium for one night before cell seeding avoided contact of the cells with the highest doses of early released Sr (Figure 11).

These results show the beneficial effects of low doses of strontium released (<8 mg/day/g of cement) on cell proliferation and differentiation that were closely related to the sustained release of strontium from Sr-loaded vaterite-DCPD cements.

In addition, we used human bone marrow stromal cells that were driven to osteogenic differentiation by dexamethasone (inductive factor), and then cultured in IMDM medium. The other papers published in the literature used different cell lines including transformed cell lines cultured in basic medium such as αMEM. The sensitivity of these differentiated cells could be different depending on the length of culture and the release of strontium within the medium in contact with these Sr-loaded cements.

CONCLUSION

Strontium is a biocompatible and bioactive element that can be introduced either as $SrCO_3$ in the solid phase or as $SrCl_2 \cdot 6H_2O$ dissolved in the liquid phase for the preparation of original vaterite $CaCO_3$-DCPD cement compositions. We showed that the various cement compositions obtained led to different release and dissolution behaviors, in agreement with the solubility of the constituting phases of the set cement (vaterite and apatite or strontium-substituted apatites). The *in vitro* release test at 37°C and the cell culture studies demonstrated that there was an initial burst of release of strontium in the medium, (highest for the SrL cement) followed by a sustained release over 3 weeks, which did not have a deleterious effect on human osteoprogenitor cell activity. The expression of an early bone marker (alkaline phosphatase) and a later bone marker (osteocalcin), which levels were overexpressed after 15 days of cell culture, was not significantly affected by the presence of strontium either within the cements or released into the medium. However, the enhanced proliferation of human osteoprogenitor cells was observed after 15 days of culture in contact with the SrS cement, which appeared to be the most promising bioactive cement composition. Interestingly, this study showed that the sustained release of Sr^{2+}, the cement biodegradation rate and the biological activity could be optimized by controlling the route of introduction of strontium into the cement paste.

REFERENCES

1. Dahl SG, Allain P, Marie PJ, Mauras Y, Boivin G, Ammann P, Tsouderos Y, Delmas PD, Christiansen C. Incorporation and distribution of strontium in bone. Bone 2001;28:446–453.
2. Pors Nielsen S. The biological role of strontium. Bone 2004;35: 583–588.
3. Marie PJ, Ammann P, Boivin G, Rey C. Mechanisms of action and therapeutic potential of strontium in bone. Calcified Tissue Int 2001;69:121–129.
4. Bonnelye E, Chabadel A, Saltel F, Jurdic P. Dual effect of strontium ranelate: Stimulation of osteoblast differentiation and inhibition of osteoclast formation and resorption in vitro. Bone 2008;42: 129–138.
5. Li C, Paris O, Siegel S, Roschger P, Paschalis EP, Klaushofer K, Fratzl P. Strontium is incorporated into mineral crystals only in newly formed bone during strontium ranelate treatment. J Bone Miner Res 2010;25:968–975.

6. Panzavolta S, Torricelli P, Sturba L, Bracci B, Giardino R, Bigi A. Setting properties and in vitro bioactivity of strontium-enriched gelatin-calcium phosphate bone cements. J Biomed Mater Res A 2008;84:965–972.
7. Yang X, Gan Y, Gao X, Zhao L, Gao C, Zhang X, Feng Y, Ting K, Gou Z. Preparation and characterization of trace elements-multidoped injectable biomimetic materials for minimally invasive treatment of osteoporotic bone trauma. J Biomed Mater Res A 2010;95:1170–1181.
8. Pina S, Vieira SI, Rego P, Torres PM, da Cruz e Silva OA, da Cruz e Silva EF, Ferreira JM. Biological responses of brushite-forming Zn- and ZnSr- substituted beta-tricalcium phosphate bone cements. Eur Cell Mater 2010;20:162–177.
9. Braux J, Velard F, Guillaume C, Bouthors S, Jallot E, Nedelec JM, Laurent-Maquin D, Laquerrière P. A new insight into the dissociating effect of strontium on bone resorption and formation. Acta Biomater 2011;7:2593–2603.
10. Banerjee SS, Tarafder S, Davies NM, Bandyopadhyay A, Bose S. Understanding the influence of MgO and SrO binary doping on the mechanical and biological properties of beta-TCP ceramics. Acta Biomater 2010;6:4167–4174.
11. Capuccini C, Torricelli P, Boanini E, Gazzano M, Giardino R, Bigi A. Interaction of Sr-doped hydroxyapatite nanocrystals with osteoclast and osteoblast-like cells. J Biomed Mater Res A 2009;89:594–600.
12. Xue W, Hosick HL, Bandyopadhyay A, Bose S, Ding C, Luk KDK, Cheung KMC, Lu WW. Preparation and cell-materials interactions of plasma sprayed strontium-containing hydroxyapatite coating. Surf Coat Technol 2007;201:4685–4693.
13. Alkhraisat MH, Moseke C, Blanco L, Barralet JE, Lopez-Carbacos E, Gbureck U. Strontium modified biocements with zero order release kinetics. Biomaterials 2008;29:4691–4697.
14. Yang L, Perez-Amodio S, Barrère-de Groot FYF, Everts V, van Blitterswijk CA, Habibovic P. The effects of inorganic additives to calcium phosphate on in-vitro behavior of osteoblasts ans osteoclasts. Biomaterials 2010;31:2976–2989.
15. Bracci B, Torricelli P, Panzavolta S, Boanini E, Giardino R, Bigi A. Effect of Mg(2+), Sr(2+), and Mn(2+) on the chemico-physical and in vitro biological properties of calcium phosphate biomimetic coatings. J Inorg Biochem 2009;103:1666–1674.
16. Marie PJ. Strontium ranelate: A physiological approach for optimizing bone formation and resorption. Bone 2006;38:S10–S14.
17. Cohen-Solal M. Strontium overload and toxicity: impact on renal osteodystrophy. Nephrol Dial Tranplant 2002;17:30–34.
18. O'Sullivan C, O'Hare P, O'Leary ND, Crean AM, Ryan K, Dobson AD, O'Neill L. Deposition of substituted apatites with anticolonizing properties onto titanium surfaces using a novel blasting process. J Biomed Mater Res B Appl Biomater 2010;95:141–149.
19. Li Y, Li Q, Zhu S, Luo E, Li J, Feng G, Liao Y, Hu J. The effect of strontium-substituted hydroxyapatite coating on implant fixation in ovariectomized rats. Biomaterials 2010;31:9006–9014.
20. Landi E, Sprio S, Sandri M, Celotti G, Tampieri A. Development of Sr and CO_3 co-substituted hydroxyapatites for biomedical applications. Acta Biomater 2008;4:656–663.
21. Wang X., Ye J., Wang Y. Influence of a novel radiopacifier on the properties of an injectable calcium phosphate cement. Acta Biomater 2007;3:757–763.
22. Jegou Saint-Jean S, Camiré CL, Nevsten P, Hansen S, Ginebra MP. Study of the reactivity and *in vitro* bioactivity of Sr-substituted α-TCP cements. J Mater Sci Mater Med 2005;16;993–1001.
23. Ni GX, Lin JH, Chiu PK, Li ZY, Lu WW. Effect of strontium-containing hydroxyapatite bone cement on bone remodeling following hip replacement. J Mater Sci Mater Med 2010;21:377–384.
24. Dagang G, Kewei X, Yaxiong L. Physicochemical properties and cytotoxicities of Sr-containing biphasic calcium phosphate bone scaffolds. J Mater Sci Mater Med 2010;21:1927–1936.
25. Wu C, Ramaswamy Y, Kwik D, Zreiqat H. The effect of strontium incorporation into $CaSiO_3$ ceramics on their physical and biological properties. Biomaterials 2007;28:3171–3181.
26. Romieu G, Garric X, Munier S, Vert M, Boudeville P. Calcium-strontium mixed phosphate as novel injectable and radio-opaque hydraulic cement. Acta Biomater 2010;6:3208–3215.
27. Combes C, Bareille R, Rey C. Calcium carbonate-calcium phosphate mixed cement compositions for bone reconstruction. J Biomed Mater Res A 2006;79:318–328.
28. Tadier S, Le Bolay N, Girod Fullana S, Cazalbou S, Charvillat C, Labarrère M, Boitel D, Rey C, Combes C. Co-grinding significance for calcium carbonate-calcium phosphate mixed cement. Part II: effect on cement properties. J Biomed Mater Res Part B 2011 (accepted).
29. Lutterotti L. Total pattern fitting for the combined size-strain-stress-texture determination in thin film diffraction. Nucl Inst Meth Phys Res B 2010;268:334–340.
30. Kamhi SR. On the structure of vaterite, $CaCO_3$, locality: synthetic. Acta Cryst 1963;16:770–772.
31. Sudarsanan K, Young RA. Significant precision in crystal structural details. Holly Springs hydroxyapatite. Acta Cryst 1969;B25:1534.
32. Vilamitjana-Amédée J, Bareille R, Rouais F, Harmand MF. Human bone marrow stromal cells express an osteoblastic phenotype in culture. In vitro Cell Dev Biol Anim 1993;29A:699–707.
33. Villars F, Guillotin B, Amédée T, Dutoya S, Bordenave L, Bareille R, Amédée J. Effect of HUVEC on human osteoprogenitor cell differentiation needs heterotypic gap junction communication. Am J Physiol Cell Physiol 2002;282:C775–C785.
34. Mosmann T. Rapid colorimetric assay for cellular growth and survival: Application to proliferation and cytotoxicity assays. J Immunol Method 1983;65:55–63.
35. Leroux L, Frèche M, Lacout JL. Calcium phosphate cement to prepare Sr-containing biomaterials. Key Eng Mater 2001;192/195: 235–238.
36. Bohner M. Design of ceramic-based cements and putties for bone graft substitution. Eur Cells Mater 2010;20:1–12.
37. Guo D, Xu K, Zhao X, Han Y. Development of a strontium-containing hydroxyapatite bone cement. Biomaterials 2005;26: 4073–4083.
38. Alkhraisat MH, Marino FT, Rodriguez CR, Jerez LB, Lopez-Carbacos E. Combined effect of strontium and pyrophosphate on the properties of brushite cements. Acta Biomater. 2008;4:664–670.
39. Wang X, Ye J. Variation of crystal structure of hydroxyapatite in calcium phosphate cement by the substitution of strontium ions. J Mater Sci Mater Med 2008;19:1183–1186.
40. O'Donnell MD, Fredholm Y, de Rouffignac A, Hill RG. Structural analysis of a series of strontium-substituted apatites. Acta Biomater 2008;4:1455–1464.
41. Christoffersen J, Christoffersen MR, Kolthoff N, Bärenholdt O. Effects of strontium ions on growth and dissolution of hydroxyapatite and on bone mineral detection. Bone 1997;20:47–54.
42. Ratier A, Freche M, Lacout JL, Rodriguez F. Behaviour of an injectable calcium phosphate cement with added tetracycline. Int J Pharm 2004;274:261–268.
43. Li RH, Bouxsein ML, Blake CA, D'Augusta D, Kim H, Li XJ, Wozney JM, Seeherman HJ. rhBMP-2 injected in a calcium phosphate paste (alpha-BSM) accelerates healing in the rabbit ulnar osteotomy model. J Orthop Res 2003;21:997–1004.
44. Alkhraisat MH, Rueda C, Cabrejos-Azama J, Lucas-Aparicio J, Mariño FT, Torres García-Denche J, Jerez LB, Gbureck U, Cabarcos EL. Loading and release of doxycycline hyclate from strontium-substituted calcium phosphate cement. Acta Biomater 2010; 6:1522–1528.
45. Schnitzler V, Fayon F, Despas C, Khairoun I, Mellier C, Rouillon T, Massiot D, Walcarius A, Janvier P, Gauthier O, Montavon G, Bouler JM, Bujoli B. Investigation of alendronate-doped apatitic cements as a potential technology for the prevention of osteoporotic hip fractures: critical influence of the drug introduction mode on the in vitro cement properties. Acta Biomater 2011;7:759–770.
46. Fernández M, Méndez JA, Vázquez B, San Román J, Ginebra MP, Gil FJ, Manero JM, Planell JA. Acrylic-phosphate glasses composites as self-curing controlled delivery systems of antibiotics. J Mater Sci Mater Med 2002;13:1251–1257.
47. Higuchi T. Mechanism of sustained action medication: theoretical analysis of rate of release of solid drugs dispersed in solid matrices. J Pharm Sci 1963;52:1145–1149.
48. Cazalbou S, Eichert D, Ranz X, Drouet C, Combes C, Harmand MF, Rey C. Ion exchanges in apatites for biomedical application. J Mater Sci Mater Med 2005;16:405–409.
49. Pan HB, Li ZY, Lam WM, Wong JC, Darvell BW, Luk KDK, Lu WW. Solubility of strontium-substituted apatite by solid titration. Acta Biomater 2009;5:1678–1685.